Dyes and Pigments 187 (2021) 109072

Contents lists available at ScienceDirect

Dyes and Pigments

journal homepage: http://www.elsevier.com/locate/dyepig

Synthesis and application of new 3-amino-2-pyridone based luminescent dyes for ELISA

Anton Shatsauskas [a], Yuri Shatalin [b], Victoria Shubina [b], Yuri Zablodtskii [c], Sergei Chernenko [a,c], Anna Samsonenko [c], Anastasiya Kostyuchenko [c], Alexander Fisyuk [a,*]

[a] Laboratory of New Organic Materials, Omsk State Technical University, 11 Mira Ave, 644050, Omsk, Russia
[b] Institute of Theoretical and Experimental Biophysics of the Russian Academy of Sciences, Institutskaja Str., 3, 142290, Pushchino, Russia
[c] Department of Organic Chemistry, Omsk F.M. Dostoevsky State University, 55a Mira Ave, 644077, Omsk, Russia

ARTICLE INFO

Keywords:
Enzyme immunoassay
3-Aminopyridin-2(1H)-One
Luminescent dye
Antioxidant activity
Horseradish peroxidase

ABSTRACT

A series of new 3-amino-4-arylpyridin-2(1*H*)-one derivatives was synthesized on the basis of oxazolo[5,4-b]pyridin-2(1*H*)-ones. Their photophysical properties and antioxidant activity were studied. Effective luminophores with an photoluminescence yield of up to 0.76 and substances exhibiting antioxidant activity exceeding ascorbic acid were revealed. It was found that the obtained luminescent dyes are horseradish peroxidase substrates and can be used to develop a rather sensitive ELISA method. The detection limits of hydrogen peroxide and horseradish peroxidase in the system containing the tested dyes lie in the nanomolar concentration range.

1. Introduction

Currently, sensitive methods for detecting viral infection are of particular importance due to pandemic caused by the coronavirus COVID-19. Methods of enzyme-linked immunosorbent assay (ELISA) are widely used to diagnose human viral diseases. This group of methods is based on the detection of a complex formed as a result of the interaction of antigens with antibodies conjugated with a tag enzyme. The presence and quantity of antigens is judged by the color change of the enzyme-sensitive substance (substrate) with which the complex is treated. One of the most frequently used enzymes in ELISA catalyzing substrate oxidation is horseradish peroxidase (HRP) [1–11]. This is due to its low cost, high catalytic activity, stability, and ease of detection of the reaction products. The most frequently used type of HRP substrates are substances, the oxidation of which results in the formation of colored compounds. Examples of such organometallic compounds include 5-aminosalicylic acid [12], 3,3′,5,5′-tetramethylbenzidine (TMB) [13], 2,2′-azinobis(3-ethylbenzothiazoline-6-sulfonic acid) (ABTS) [14] and others. As a rule, these peroxidase substrates have a lower sensitivity compared to substrates whose oxidation products fluoresce [15]. Examples of such substrates are dihydroxyphenoxazine derivatives (10-acetyl-3,7-dihydroxyphenoxazine, Amplex Red) and tyramide [16]. However, at a low concentration of the target molecules, a long time of incubation of substrates in the presence of hydrogen peroxide and immobilized peroxidase is required. Sometimes this leads to a misrepresentation of the analysis results due to the complex kinetics of the enzymatic reaction. For a more accurate assessment, it is necessary to take into account the inhibition and inactivation of peroxidase over time, as well as the side reactions of the fluorescent substrate, etc. The use of substrates that lose their fluorescent properties during oxidation process can make it possible to more accurately estimate the amount of immobilized peroxidase from the descending kinetic dependence of the fluorescent dye oxidation.

Earlier, we have developed methods for the synthesis of 4-aryl-3-amonopyridin-2(1*H*)-ones [17–25], which turned out to be effective luminophores. When studying the antioxidant activity of these compounds, we noticed that they are easily oxidized, they lose luminescent properties upon oxidation and therefore are of interest as dyes for ELISA. Data on amino-substituted derivatives of 3-amino-4-arylpyridin-2(1*H*)-ones, their methods of preparation and luminescent properties are scarce.

The aim of this work is to synthesize 3-amino-4-arylpyridin-2(1*H*)-one derivatives, to study their photophysical properties, and also to search for luminescent dyes among them, which can be used as new luminescent HRP substrates in ELISA.

* Corresponding author.
E-mail address: fisyuk@chemomsu.ru (A. Fisyuk).

https://doi.org/10.1016/j.dyepig.2020.109072
Received 20 October 2020; Received in revised form 5 November 2020; Accepted 6 December 2020
Available online 16 December 2020

2. Results and discussion

2.1. Synthesis of 3-amino-4-arylpyridin-2(1H)-one derivatives

Recently, we have developed a simple method for the synthesis of oxazolo[5,4-*b*]pyridin-2(1*H*)-ones **1**–**3** [20,25]. These compounds, as well as the *N*-alkylation products **7a–d**, **7i** obtained by interaction of oxazolo[5,4-*b*]pyridin-2(1*H*)-one **1** with alkyl halides, were used as starting materials for the preparation of 4-phenyl-3-amonopyridin-2(1*H*)-ones **8a–c**, **8e**, **8i**, **9**. The reaction of (2-bromoethyl)-5-methyl-7--phenyloxazolo[5,4-*b*]pyridin-2(1*H*)-one **7d** (R = CH_2Br) with 2-(2-(2-methoxyethoxy)ethoxy)ethan-1-ol in the presence of NaH in DMF furnished podand **7j**. Heating oxazolo[5,4-*b*]pyridin-2(1*H*)-ones **1**–**3**, **7a–c**, **7j** with alkali in water or water–dioxane (1:1) mixture led to hydrolysis of the oxazole ring and the formation of 3-amino-4--arylpyridin-2(1*H*)-ones **4**–**6**, as well as their *N*-substituted derivatives **8a–c**, **8j**.

Methyl-3-(methylamino)-4-phenylpyridin-2(1*H*)-one **8h** and 3-(ethyl(methyl)amino)-6-methyl-4-phenylpyridin-2(1*H*)-one **9** were obtained by reduction of oxazolo[5,4-*b*]pridin-2(1*H*)-ones **1** and **7i** with sodium borohydride in the presence of trifluoroacetic acid or $AlCl_3$ in THF (Scheme 1). The reaction of 3-amino-6-methyl-4-phenylpyridin-2(1*H*)-one **4** and aromatic aldehydes (benzaldehyde, thiophenecarbaldehyde, and furfural) with $NaBH_4$ in the presence of formic acid led to the formation of 3-alkylamino-4-arylpyridin-2(1*H*)-ones **8e–g** in 78–87% yield. Previously, these compounds have been prepared through a two-step process including the isolation of intermediate Schiff bases [22].

Since oxazolo[5,4-*b*]pyridin-2(1*H*)-ones **1**–**3**, **7** underwent the alkali-induced ring opening, we studied their reactions with nucleophiles. Thus, the reactions of compound **4** with alcohols, ammonia, or amines upon heating resulted in the opening of the five-membered ring to form carbamates **10**, **11** and ureas **12**–**16** in 56–72% and 60–71% yields, respectively. Amide **17** was obtained by acylation of 3-amino-2-pyridone **4** as described in ref. [18].

Thus, we obtained a series of 3-amino-4-arylpyridin-2(1*H*)-ones bearing various substituents at the nitrogen atom. Some of them are readily soluble in water (**8a**, **10**–**16**), alcohols (**4**–**6**, **8a–c**, **8e**, **8h**, **8j**, **9**–**16**) and non-polar solvents (**4**–**6**, **8a–c**, **8e**, **8h**, **8j**, **9**).

2.2. Photophysical properties of 3-amino-4-arylpyridin-2(1H)-one derivatives and their antioxidant activity

In order to select the most promising substrates for ELISA, the photophysical properties and antioxidant activity of the synthesized compounds were studied. UV and fluorescence spectra were recorded for alcohol solutions of compounds **4**–**6**, **8a–c**, **8e–h**, **8j**, **9**–**17**, the light absorption coefficient and the quantum fluorescence yield were calculated. In the absorption spectra of 3-amino-4-arylpyridin-2(1*H*)-ones derivatives **4**–**6** there are two main absorption bands with maxima in <251 and 320–351 nm regions, corresponding to π–π* and n–π* transitions. The emission maxima lie in the 420–451 nm range, and the luminescence quantum yield reaches 0.76 (**4**). The luminescence quantum yield decreases when the phenyl substituent at the C^4 atom is replaced by substituted aryl (**5**, Φ_{fl} = 0.50) or thiophene moiety (**6**, Φ_{fl} = 0.37). Substituent at the nitrogen atoms (**8a–c**, **8e–h**, **8j**, **9**) also leads to a decrease in the quantum yield to 0.43–0.63 (**8a–c**, **8e–h**) and to 0.05 in the case of the presence of two alkyl groups (**9**). For carbamates **10**, **11** and ureas **12**–**16**, a hypsochromic shift is observed in the absorption and luminescence spectra. The absorption maxima in UV and luminescence spectra are in the 317–323 and 420–440 nm region, respectively.

The quantum yields of compounds **10**–**17** also lie in the range of

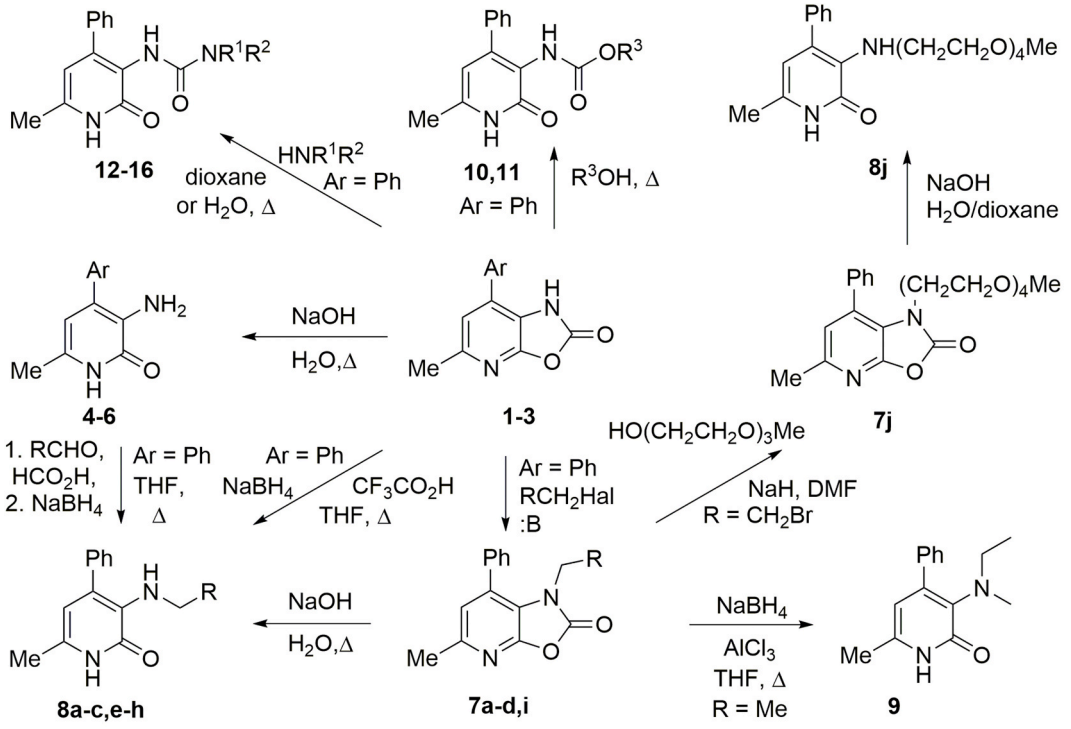

1,4 Ar = Ph; **2,5**.Ar = C_6H_3-3,4-$(OMe)_2$; **3,6** Ar = 2-Th; **10** R^3 = Et, **11** R^3 = *i*-Pr; **12** R^1= R^2 = H; **13** R^1= Me, R^2= H; **14** R^1= Bn, R^2 = H; **15** R^1 = Ph, R^2 = H; **16** R^1 + R^2 = $(CH_2CH_2)_2O$; **a** R = CH_2OH; **b** R= $CH_2OCH_2CH_2OMe$; **c** R= $CH_2O(CH_2CH_2O)_2Me$; **d** R = CH_2Br; **e** R = 2-Fur; **f** R = 2-Th; **g** R = Ph; **h** R = H; **i** R = Me.

Scheme 1. Synthesis of 3-amino-4-arylpyridin-2(1H)-one derivatives.

0.11–0.31. It should be noted that, for all the studied compounds, a sufficiently large Stokes shift (98–114 nm) is observed, and in the case of dialkyl amine **9** it reaches 172 nm (Table 1). UV spectra of compounds **8a–c**, **8e–h**, **8j**, **9–17** are presented in Supplementary Material (Table SB1, Figures SB1–SB5).

The antioxidant activity (AOA) of 3-amino-4-arylpyridin-2(1*H*)-ones derivatives **8a–c**, **8e**, **8h**, **8j**, **9–17** was studied by a modified FRAP method based on the spectrophotometric determination of the Fe^{2+}–2,2′-bipyridyl complex obtained by reduction of ferric iron with an antioxidant in the presence of 2,2′-bipyridyl [31,32] for 15 min. The AOA of the tested fluorescent dyes (FD) was assessed relative to ascorbic acid (AA) according to the calibration graph (SM, Table SC1–SC3, Figures SC1–SC3). The results obtained are shown in Table 1 and are expressed as the equivalent antioxidant activity of ascorbic acid ([FD]/[AA]). It was shown that the AOA of 3-amino-2-pyridones **4–6**, **8a–c**, **8e–h**, **8j** is comparable to activity of ascorbic acid, and some compounds are superior in activity to ascorbic acid. It should be noted that the introduction of an electron-withdrawing substituent to the amino group leads to a drop in AOA, which for compounds **10–17** is 0.02–0.12. The activity of *N*-dialkyl-substituted 3-amino-2-pyridone **9** also turned out to be low (0.24). Among the 3-amino-4-arylpyridin-2(1*H*)-one derivatives, which have better antioxidant activity and luminescent properties, compounds **4–6**, **8a**, **8e**, **8j** differing in the structure of the aryl moiety and the substituent at the nitrogen atom were selected for further studies. It was found that the concentration dependence of the fluorescence intensity of these compounds in water remains linear up to 100 μM (Fig. 1).

No oxidation of aqueous solutions of 3-amino-4-arylpyridin-2(1*H*)-ones **4–6**, **8a**, **8e**, **8j** was observed when standing in air for 24 h at room temperature. The results obtained indicate the absence of self-quenching, aggregation, and sufficient stability of these compounds, which makes it possible to calibrate their aqueous solutions.

2.3. Oxidation of 3-amino-4-arypyridin-2(1*H*)-ones with H_2O_2 in the presence of horseradish peroxidase

Most of the simplest derivatives of phenol and aniline can be oxidized by hydrogen peroxide in the presence of HRP [33]. It could be assumed that 3-amino-4-arylpyridin-2(1*H*)-ones derivatives will be oxidized in a similar way (Scheme 2).

Indeed, the luminescent properties of solutions of the studied dyes **4–6**, **8a**, **8e**, **8j** in the presence of hydrogen peroxide at a concentration of 500 μM did not change practically. Whereas in the presence of HRP and hydrogen peroxide, a decrease in the fluorescence intensity of

Table 1
Photophysical properties and antioxidant activity of compounds 4–6, 8a–c, 8e–h, 8j, 9–17.

№	Fluorescent dye	Ar, X or R^1,R^2	UV–Vis[a]		Photoluminescence[b]					AOA = mol(FD)/mol (AA)[c]
			$^{max}\lambda_{abs}$ [nm]	ε, 10^3 [l/cm*mol]	λ_{ex}[nm]	$^{max}\lambda_{em}$ [nm]	Stokes shift [nm]	Stokes shift [eV]	Quantum yield (Φ_{fl})[b]	
4	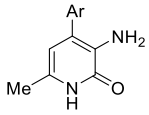	Ph	334	8.9	335; 350	435	101	0.86	0.76 ± 0.03	0.94 ± 0.04
5		C_6H_3-3,4-$(OMe)_2$	334	9.8	335; 350	437	103	0.88	0.50 ± 0.02	0.97 ± 0.02
6		Thienyl	351	8.3	350; 355	451	100	0.78	0.37 ± 0.01	1.17 ± 0.03
8a	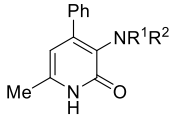	H, CH_2CH_2OH	338	6.9	340; 350	447	109	0.89	0.53 ± 0.02	0.91 ± 0.01
8b		H, $(CH_2CH_2O)_2Me$	337	8.8	340; 350	448	111	0.91	0.55 ± 0.02	0.94 ± 0.01
8c		H, $(CH_2CH_2O)_3Me$	336	7.7	325; 335	449	113	0.93	0.58 ± 0.02	0.95 ± 0.03
8e		H, CH_2-2-Furyl	339	8.8	330; 340	447	108	0.89	0.39 ± 0.01	1.13 ± 0.05
8f		H, CH_2-2-Thienyl	338	7.8	330; 340	448	110	0.90	0.44 ± 0.01	1.16 ± 0.04
8g		H, Bn	337	7.0	330; 340	452	115	0.94	0.44 ± 0.01	1.11 ± 0.04
8h		H, Me	340	9.3	340; 350	445	105	0.86	0.43 ± 0.02	0.95 ± 0.03
8j		H, $(CH_2CH_2O)_4Me$	329	9.7	330; 340	443	114	0.93	0.62 ± 0.03	1.14 ± 0.01
9		Me, Et	320	4.3	320; 330	492	172	1.35	0.05 ± 0.00	0.24 ± 0.01
10	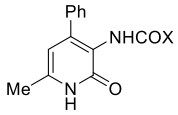	EtO	317	8.1	310; 320	424	107	0.99	0.11 ± 0.00	0.09 ± 0.01
11		i-PrO	319	6.1	310; 320	427	108	0.99	0.14 ± 0.01	0.06 ± 0.01
12		NH_2	319	4.8	310; 320	420	101	0.96	0.12 ± 0.00	0.02 ± 0.01
13		NHMe	317	5.5	310; 320	424	107	0.97	0.21 ± 0.01	0.04 ± 0.01
14		NHBn	318	6.4	310; 320	428	110	1.00	0.28 ± 0.01	0.07 ± 0.01
15		NHPh	323	5.5	310; 320	440	117	1.02	0.31 ± 0.01	0.05 ± 0.01
16		$N(CH_2CH_2)_2O$	318	5.2	310; 320	425	107	0.98	0.31 ± 0.01	0.06 ± 0.01
17		Me	333	7.0	330; 340	431	98	0.85	0,16 ± 0.01	0.12 ± 0.01

[a] EtOH was used as a solvent (10^{-7}–10^{-5} mol/l).
[b] The fluorescence quantum yield was calculated relative to the standard (quinine sulfate in 0.5 M H_2SO_4, Φ_{fl} = 0.546) [26–30].
[c] The antioxidant activity (AOA) of the studied compounds (FD) was assessed by the FRAP method relative to the standard ascorbic acid (AA) [31,32].

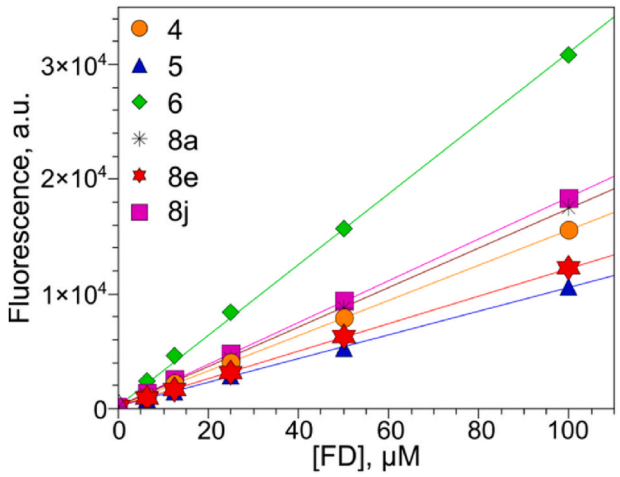

Fig. 1. The concentration dependence of fluorescence intensity of compounds **4–6**, **8a**, **8e**, **8j**.

solutions of these compounds was observed, which indicates their oxidation. The oxidation rate of the tested compounds linearly depended on the enzyme concentration (Fig. 2). This indicates that the studied compounds are HRP substrates.

To determine the stoichiometry of HRP-catalyzed oxidation of 3-amino-4-arylpyridin-2(1*H*)-ones **4–6**, **8a**, **8e**, **8j** with hydrogen peroxide, the following experiments were carried out: a solution of hydrogen peroxide was successively added to 1 and 100 μM solutions of tested compounds. The final concentration of hydrogen peroxide varied from 10 nM to 1 μM in the first case and from 1 μM to 100 μM in the second.

In both cases, the fluorescence intensity rapidly decreased and reached a certain constant value after adding each new aliquot, which indicates a rapid consumption of hydrogen peroxide. At the same time, the relative fluorescence intensity (I/I_0) of compounds **4–6**, **8a**, and **8e** linearly depended on the concentration of hydrogen peroxide (as well as the molar ratio of hydrogen peroxide/dye) (SM, Figure SD1). As an example, Fig. 3 shows the change in the fluorescence intensity of compound **6** during titration with hydrogen peroxide and the obtained $I/I_0 = f([H_2O_2])$ dependence for this compound.

The dependence of the change in the molar concentration of compounds **4–6**, **8a**, and **8e** on the molar concentration of hydrogen peroxide added to the system was also linear (Fig. 4). The slope of the tangent, equal to the desired stoichiometric ratio $[FD]/[H_2O_2]$, was practically the same for these compounds and was close to 1 (Fig. 4).

At the same time, the amount of hydrogen peroxide required for the oxidation of compound **8j** was higher than those of compounds mentioned above (Fig. 4). In addition, for compound **8j** at a concentration of 100 μM, two linear regions can be distinguished, whereas at a concentration of 1 μM, one linear curve was observed. Apparently, the oxidation of compound **8j** involved not only the heterocycle, but also the substituent at the nitrogen atom, which makes its use as a horseradish peroxidase substrate inappropriate. The coefficients of the linear regression equations for the above relationships for compounds **4–6**, **8a**, and **8e** are given in Supplementary Material (SM, Table SD1).

Limit of detection (LOD) is one of the important parameters of ELISA method [34]. This parameter is the minimum amount of the analyte in the sample, the signal from which can be reliably distinguished from the background. The calculation of the detection limits for hydrogen peroxide in the HRP-catalyzed oxidation of compounds **4–6**, **8a**, and **8e** was performed on the basis of the data obtained by titrating 1 μM solutions of the tested compounds with a hydrogen peroxide solution (SM, Figure SD1). Since the fluorescence intensity of the solution quickly reached a stationary level during titration after the addition of each new aliquot of peroxide (Fig. 3), the limit of detection for H_2O_2 was calculated using the standard deviation of the fluorescence signal [35,36].

To determine the limit of detection for HRP, HRP at various concentrations was added to solutions containing fluorescent dyes **4–6**, **8a**, **8e**, and H_2O_2. The mixtures were incubated at 37 °C for 15 min, then the fluorescence was recorded. As shown in Fig. 5, there was a linear dependence of the change in the concentration of the dye on the concentration of HRP. However, the kinetics of oxidation of dyes at different concentrations of HRP was different. In this regard, the RMSE method was used to determine the limit of detection for HRP [37]. The results are collected in Table 2.

In conclusion, the detection limits of hydrogen peroxide and horseradish peroxidase in systems containing the tested compounds are approximately the same as for the dyes used in ELISA kits, and lie in the range of nanomolar concentrations. Therefore, the obtained compounds can be used to develop a rather sensitive method for the determination of hydrogen peroxide and, in the future, to modify ELISA method.

3. Materials and methods

3.1. General information

All chemicals and solvents were purchased from commercial suppliers and used as granted. Crude products were purified by column chromatography with silica gel (100–200 mesh) or recrystallization. The reaction progress and purity of the products were monitored by thin layer chromatography on Sorbfil UV-254 plates which were visualized

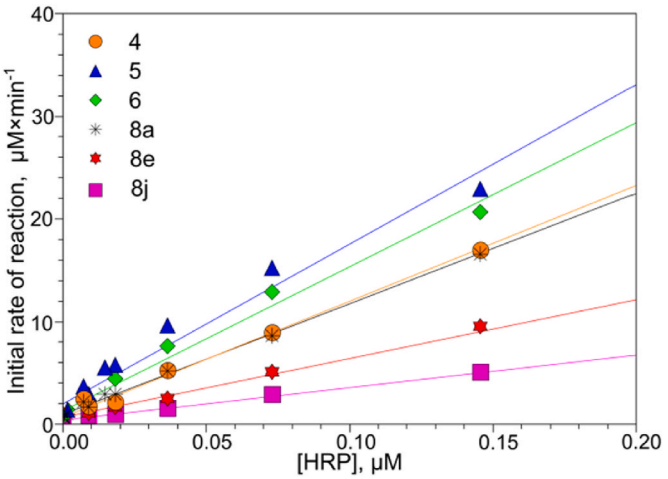

Fig. 2. Dependence of the initial rate of oxidation of fluorescent dyes (FD) on the horseradish peroxidase concentration (HRP).

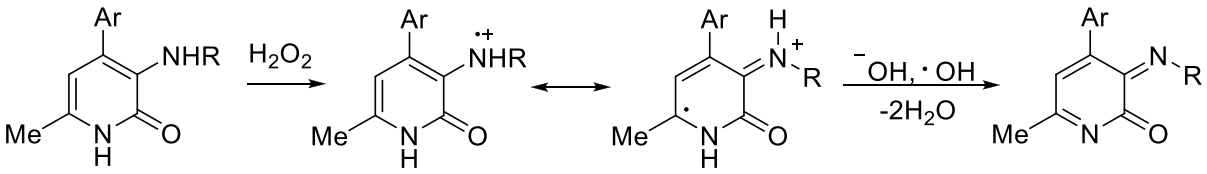

Scheme 2. Oxidation of 3-amino-4-arypyridin-2(1H)-ones.

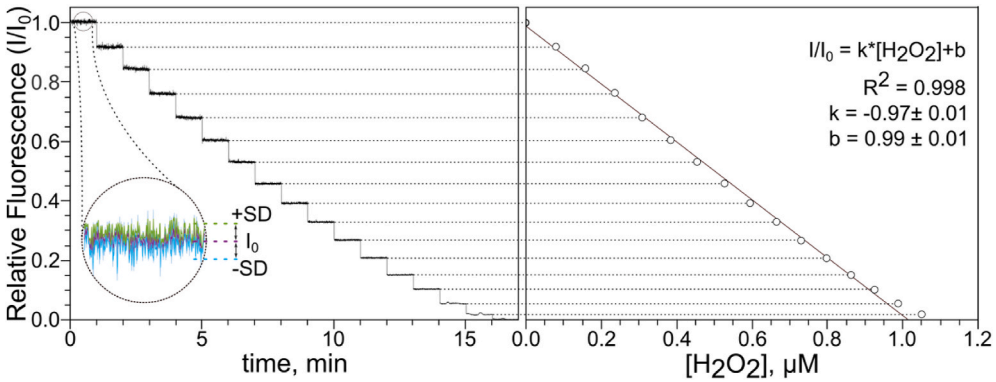

Fig. 3. Change in the relative fluorescence intensity of dye **6** upon successive addition of hydrogen peroxide. Left – titration curve; right – relative intensity of dye fluorescence depending on the concentration of added hydrogen peroxide. C_0(**6**) = 1 μM.

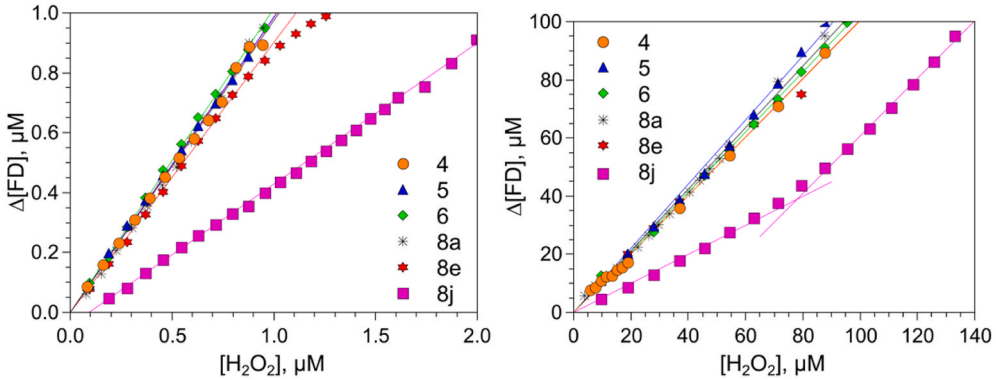

Fig. 4. Changes in the concentration of fluorescent dyes depending on the concentration of hydrogen peroxide. The initial concentration of the dyes was 1 μM (left) and 100 μM (right).

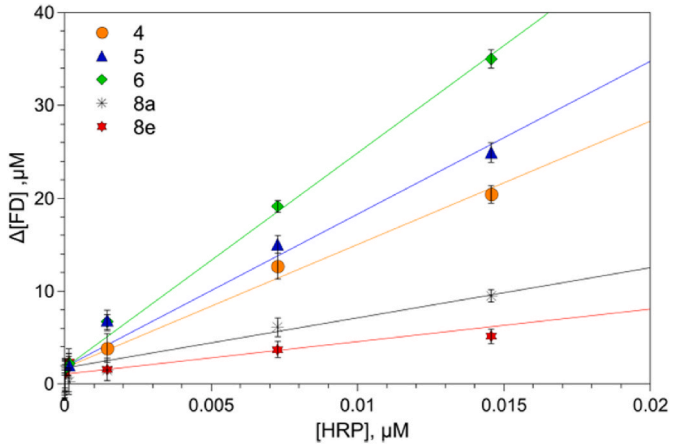

Fig. 5. Changes in the concentration of fluorescent dyes (FD) depending on the concentration of horseradish peroxidase (HRP). The initial concentration of fluorescent dyes was 100 μM, and the concentration of hydrogen peroxide was 50 μM.

with UV light (254, 365 nm). All chemicals were of analytical grade and purchased from Sigma-Aldrich Chemical Co.

The ^{1}H and ^{13}C NMR spectra were recorded on a Bruker Avance Instrument operating at 400 MHz and 100 MHz for ^{1}H and ^{13}C nuclei, respectively. Chemical shifts are referenced relative to TMS or the residual signals of protonated solvents as an internal standard: chloroform (δ = 7.26 (1) in ^{1}H NMR, δ = 77.00 (3) in ^{13}C NMR), DMSO-d_6 (δ = 2.49 (5) in ^{1}H NMR, δ = 39.5 (7) in ^{13}C NMR). Most of the ^{13}C NMR spectra were obtained in the *J*-modulation mode.

Table 2
Limits of detection for hydrogen peroxide and horseradish peroxidase.

Fluorescent dye	LOD_{H2O2}, nM	LOD_{HRP}, nM
4	8.97 ± 1.01	2.45 ± 0.45
5	7.78 ± 3.75	3.40 ± 1.06
6	3.17 ± 0.70	1.58 ± 0.44
8a	11.45 ± 4.61	2.92 ± 0.63
8e	6.84 ± 2.79	7.45 ± 2.19

The IR spectra were recorded on Infralum FT-801 spectrometer from KBr pellets or thin layer.

The elemental analyses were carried out on a Carlo Erba 1106 CHN analyzer. The melting points were determined on a Reach devices RD-MP. UV–Vis spectra were taken in EtOH or DMSO (10^{-7}-10^{-5} mol/l) using a UV/VIS/NIR Spectrometer Lambda 750 (PerkinElmer), while fluorescence spectra were recorded on Cary Eclipse (Agilent) fluorescence spectrometer. Fluorescence excitation spectra were recorded to determine the excitation wavelength at which the maximum fluorescent response is observed. Subsequent fluorescence emission spectra were recorded at excitation wavelengths determined in this manner. The quantum yield of examined compounds was determined relative to quinine sulfate in 0.5 M H_2SO_4, Φ_{fl} = 0.546, using comparative method [26–30].

The antioxidant activity of the tested compounds was determined by the modified FRAP method [31,32]. Antioxidant activity was assessed relative to a standard substance (ascorbic acid) according to a calibration graph by measuring the optical density of aqueous solutions containing 1.0 ml of an alcohol solution of 2,2′-bipyridyl (c =1.2·10^{-2}

mol/l), 1.0 ml of a $FeNH_4(SO_4)_2{\cdot}12H_2O$ solution ($c = 6.0 \cdot 10^{-3}$ mol/l), and 0.5–1.00 ml of a solution of the test compound ($c = 0.1$ mg/ml) (SM, Table SC1-SC3, Figures SC1-SC3). Before studying antioxidant activity of the tested compounds, the possibility of complexation of these reagents with Fe^{2+} ions was studied. These compounds do not form complexes with Fe^{2+}, which is confirmed by the absence of significant deviations from additivity in the spectra of solutions containing the reagent and the Fe^{2+} salt (in the ratio of Fe^{2+}:R = 1:3).

3.2. Synthesis

Procedures for the syntheses of 7-aryl[1,3]oxazolo[5,4-*b*]pyridin-2(1*H*)-ones **1**–**3**, 3-amino-4-arylpyridine-2(1*H*)-ones **4**–**6**, 1-alkyl-5-methyl-7-phenyl[1,3]oxazolo[5,4-*b*]pyridin-2(1*H*)-ones **7b**, **7j**, and *N*-(6-methyl-2-oxo-4-phenyl-1,2-dihydropyridin-3-yl)acetamide **16** have been reported earlier in Ref. [18,20,25,30]. Synthesis methods and spectral data for all the synthesized compounds are presented in SM (Section A).

3.3. Study of HRP-catalyzed oxidation of luminescent dyes with hydrogen peroxide

All solutions were prepared in distilled water, additionally purified on a Milli-Q device (Millipore, USA). HRP (CAT #P8125) was purchased from Sigma-Aldrich (USA). HRP was dissolved in 20 mM phosphate-buffered saline, pH 7.4 ($A_{403}/A_{275} = 2.8$–3.0), and its concentration was determined spectrophotometrically ($\varepsilon_{403} = 100$ mM^{-1} cm^{-1}) [38]. Hydrogen peroxide (30%) was purchased from Sigma-Aldrich (USA) and its concentration was confirmed spectrophotometrically ($\varepsilon_{240} = 39.4$ M^{-1} cm^{-1} [39]).

Stock solutions of fluorescent dyes (**4**–**6**, **8a**, **8e**, **8j**) (100 mM) were prepared in DMSO and their concentrations were determined spectrophotometrically (using the extinction coefficients presented in Table 1).

Fresh solutions of fluorescent dyes, HRP, and H_2O_2 were prepared before each experiment.

3.3.1. Oxidation of fluorescent dyes

Oxidation of the tested compounds was evaluated by the decrease in the fluorescence intensity with time. Measurements were performed in 20 mM phosphate buffered saline (PBS) in the absence and presence of hydrogen peroxide at 37 °C on a Tecan Infinite F200 microplate reader (Australia) in 96 well plates (Greiner 655076). The excitation wavelength was 360 ± 12.5 nm, and the emission wavelength was 465 ± 17.5 nm. The final concentration of fluorescent dyes was 100 μM, the final concentration of hydrogen peroxide was 500 μM. In both cases, no oxidation reaction of fluorescent dyes was observed. To study the effect of HRP on the oxidation of fluorescent dyes, HRP was added to a mixture containing fluorescent dyes (at a final concentration of 100 μM) and H_2O_2 (at a final concentration of 50 μM). The final concentration of the enzyme varied from 9 to 145 nM. The initial rates were determined from the slope of the initial linear region of the kinetic curves. At least five independent experiments were performed and the mean values of the initial rates were calculated. Next, a graph was plotted of the dependence of the average values of the initial rates (converted into changes in the concentration of the fluorescent dyes) on the molar concentration of HRP.

3.3.2. Stoichiometry of HRP-catalyzed oxidation of fluorescent dyes

Stock solutions of the fluorescent dyes (**4**–**6**, **8a**, **8e**, **8j**) (100 mM) were used to prepare working solutions (1 μM and 100 μM) in PBS (pH 7.4). Then the dyes were titrated with hydrogen peroxide in the presence of HRP (SM, section D). The oxidation of the tested compounds was evaluated by the decrease in the fluorescence intensity. Measurements were performed on a Cary Eclipse spectrofluorimeter (Varian, Australia) using standard 1 cm quartz cells at room temperature using the wavelengths shown in Table 1.

The calculation of the concentrations of compounds was carried out according to the following formulas:

$$[H_2O_2] = [H_2O_2]_0 \cdot Va/(V_0+Va);$$

$$[FD] = [FD]_0 \cdot I/I_0;$$

where $[H_2O_2]$ и $[H_2O_2]_0$ – final and initial concentrations of hydrogen peroxide, respectively, μM; V_0 – initial volume of a solution containing FD and HRP; Va – additive volume of H_2O_2; [FD] and $[FD]_0$ – final and initial concentration of the fluorescent dye, respectively, μM; I – fluorescence intensity after adding hydrogen peroxide; I_0 – fluorescence intensity before addition of hydrogen peroxide.

Next, a graph was plotted as a function of the molar concentration of the compound oxidized after the addition of hydrogen peroxide versus the molar concentration of hydrogen peroxide added to the system. The stoichiometry of the HRP-catalyzed oxidation of the tested compounds with hydrogen peroxide was determined from the slope of the obtained curves.

3.3.3. Determination of the limits of detection

To determine the limit of detection of H_2O_2 by fluorimetry using fluorescent dyes **4**–**6**, **8a**, **8e**, we used the data obtained by titrating 1 μM dye solutions with a hydrogen peroxide solution. A graph was plotted as a function of the relative intensity (I/I_0) of fluorescence versus the molar ratio H_2O_2/FD. LOD_{H2O2} was calculated using the formula: $LOD_{H2O2} = 3{*}SD/k_1$ [34], where SD is the standard deviation of the fluorescence signal, k_1 is the slope of the regression line obtained for the experimental data.

To determine the limits of detection for HRP, HRP at various concentrations was added to solutions containing fluorescent dye (**4**–**6**, **8a**, **8e**) and H_2O_2 (SM, section D). The mixtures were incubated at 37 °C for 15 min, then fluorescence was recorded on a Tecan Infinite F200 microplate reader (Austria) in 96 well plates using excitation and emission wavelengths of 360 ± 12.5 and 465 ± 17.5 nm, respectively. Changes in the fluorescence intensity of compounds were converted to changes in compound concentrations. Next, a graph was plotted as a function of the molar concentration of the compound oxidized after the addition of hydrogen peroxide versus the molar concentration of HRP added to the system. LOD_{HRP} was calculated as follows [37]: $LOD_{HRP} = 3{\cdot}RMSE/k_2$, where RMSE – root mean square error of linear regression; k_2 – linear regression slope.

The calculation of standard deviations, root mean square errors of the model and slope coefficients of linear regression was carried out using the LibreOffice 6.4 Calc and QtiPlot 0.9.8.9 software packages.

Declaration of competing interest

The authors declare that they have no known competing financial interests or personal relationships that could have appeared to influence the work reported in this paper.

Acknowledgements

This work was supported by the Russian Science Foundation (Grant no. 19-13-00273).

Appendix A. Supplementary data

Supplementary data to this article can be found online at https://doi.org/10.1016/j.dyepig.2020.109072.

References

[1] Hosseini S, Vazquez-Villegas P, Rito-Palomares M, Martinez-Chapa SO. Enzymes and substrates. In: Enzyme-linked immunosorbent assay (ELISA): from A to Z. Singapore: Springer; 2018. p. 34–40.

[2] Yanga H, Zhangb Q, Liuc X, Yanga Y, Yangc Y, Liuc M, et al. Antibody-biotin-streptavidin-horseradish peroxidase (HRP) sensor for rapid and ultra-sensitive detection of fumonisins. Food Chem 2020;316:126356. https://doi.org/10.1016/j.foodchem.2020.126356.

[3] Bae Y, Jang DG, Eom S, Park TJ, Kang S. HRP-conjugated plug-and-playable IgG-binding nanobodies as secondary antibody mimics in immunoassays. Sens Actuators, B 2020;320:128312. https://doi.org/10.1016/j.snb.2020.128312.

[4] Dutta P, Shrivastav TG, Thakur SC. Homologous ELISA for measurement of medroxyprogesterone acetate in serum. Anal Biochem 2018;558:60–8. https://doi.org/10.1016/j.ab.2018.07.010.

[5] Bodulev OL, Gribas AV, IYu Sakharov. Microplate chemiluminescent assay for HBV DNA detection using 3-(10′- phenothiazinyl)propionic acid/N-morpholinopyridine pair as enhancer of HRP-catalyzed chemiluminescence. Anal Biochem 2018;543:33–6. https://doi.org/10.1016/j.ab.2017.11.026.

[6] Segura-Gil I, Nicolau-Lapena I, Galan-Malo P, Mata L, Calvo M, Sánchez L, et al. Development of two ELISA formats to determine glycinin. Application to detect soy in model and commercial processed food. Food Contr 2018;93:32–9. https://doi.org/10.1016/j.foodcont.2018.05.038.

[7] Miyashita K, Fukamachi I, Machida T, Nakajimad K, Young SG, Murakami M, et al. An ELISA for quantifying GPIHBP1 autoantibodies and making a diagnosis of the GPIHBP1 autoantibody syndrome. Clin Chim Acta 2018;487:174–8. https://doi.org/10.1016/j.cca.2018.09.039.

[8] Gonga Ch, Yu Gonga, Oo MKK, Yu Wua, Rao Yu, Tan X, Fan X. Sensitive sulfide ion detection by optofluidic catalytic laser using horseradish peroxidase (HRP) enzyme. Biosens Bioelectron 2017;96:251–7. https://doi.org/10.1016/j.bios.2017.05.024.

[9] Sajic N, Oplatowska-Stachowiak M, Streppel L, Drijfhout JW, Salden M, Koning F. Development and in-house validation of a competitive ELISA for the quantitative detection of gluten in food. Food Contr 2017;80:401–10. https://doi.org/10.1016/j.foodcont.2017.05.021.

[10] Xu W, Tian J, Shao X, Zhu L, Huang K, Luo Yu. A rapid and visual aptasensor for lipopolysaccharide detection based on the bulb-like triplex turn-on switch coupled with HCR-HRP nanostructures. Biosens Bioelectron 2017;82(2):795–801. https://doi.org/10.1016/j.bios.2016.10.012.

[11] IYu Sakharov, Demiyanova AS, Gribas AV, Uskova NA, Efremov EE, Vdovenko MM. 3-(10′-Phenothiazinyl)propionic acid is a potent primary enhancer of peroxidase-induced chemiluminescence and its application in sensitive ELISA of methylglyoxal-modified low density lipoprotein. Talanta 2013;115:414–7. https://doi.org/10.1016/j.talanta.2013.05.074.

[12] Ellens DJ, Gielkens ALJ. A simple method for the purification of 5-aminosalicylic acid. Application of the product as substrate in enzyme-linked immunosorbent assay (ELISA). J Immunol Methods 1980;37(3–4):325–32. https://doi.org/10.1016/0022-1759(80)90318-X.

[13] Yoshitake Y, Fukuma D, Yuno A, Hirayama M, Nakayama H, Tanaka T, et al. Phase II clinical trial of multiple peptide vaccination for advanced head and neck cancer patients revealed induction of immune responses and improved OS. Clin Canc Res 2015;21(2):312–21. https://doi.org/10.1158/1078-0432.CCR-14-0202.

[14] Shin KJ, Lee YJ. Purification and characterization of a new member of the laccase family from the white-rot basidiomycete Coriolus hirsutus. Arch Biochem Biophys 2000;384(1):109–15. https://doi.org/10.1006/abbi.2000.2083.

[15] Giljohann DA, Mirkin CA. Drivers of biodiagnostic development. Nature 2009;462:461–4. https://doi.org/10.1038/nature08605.

[16] Acharya AP, Nafisi PM, Gardner A, MacKay JL, Kundu K, Kumara S, et al. A fluorescent peroxidase probe increases the sensitivity of commercial ELISAs by two orders of magnitude. Chem Commun 2013;49(88):10379–81. https://doi.org/10.1039/c3cc44783a.

[17] Goncharov DS, Kostuchenko AS, Fisyuk AS. Synthesis of pyridin-2(1H)-ones by the intramolecular cyclization of amides of β-enamino ketones. Chem Heterocycl Compd 2009;45(7):793–5. https://doi.org/10.1007/s10593-009-0358-8.

[18] Fisyuk AS, Kulakov IV, Goncharov DS, Nikitina OS, Bogza YP, Shatsauskas AL. Synthesis of 3-aminopyridin-2(1H)-ones and 1H-pyrido[2,3-b][1,4]oxazin-2(3H)-ones. Chem Heterocycl Compd 2014;50(2):217–24. https://doi.org/10.1007/s10593-014-1464-9.

[19] Kulakov IV, Matsukevich MV, Shulgau ZT, Sergazy S, Seilkhanov TM, Puzari A, et al. Synthesis and antiradical activity of 4-aryl(hetaryl)-substituted 3-aminopyridin-2(1H)-ones. Chem Heterocycl Compd 2015;51(11/12):991–6. https://doi.org/10.1007/s10593-016-1809-7.

[20] Shatsauskas AL, Abramov AA, Saibulina ER, Palamarchuk IV, Kulakov IV, Fisyuk AS. Synthesis of 3-amino-6-methyl-4-phenylpyridin-2(1H)-one and its derivatives. Chem Heterocycl Compd 2017;53(2):186–91. https://doi.org/10.1007/s10593-017-2038-4.

[21] Palamarchuk IV, Matsukevich MV, Kulakov IV, Seilkhanov TM, Fisyuk AS. Synthesis of N-substituted 2-aminomethyl-5-methyl-7-phenyloxazolo[5,4-b]pyridines. Chem Heterocycl Compd 2019;55(8):788–91. https://doi.org/10.1007/s10593-019-02537-y.

[22] Kulakov IV, Palamarchuk IV, Shulgau ZT, Seilkhanov TM, Gatilov YV, Fisyuk AS. Synthesis, structure and biological activity 3-(arylmethyl) aminopyridine-2(1H)-ones and 1H-pyrido[2,3-b][1,4]oxazin-2(3H)-ones. J Mol Struct 2008;1166:262–9. https://doi.org/10.1016/j.molstruc.2018.04.036.

[23] Kulakov IV, Shatsauskas AL, Matsukevich MV, Palamarchuk IV, Seilkhanov TM, Gatilov YV, et al. A new approach to the synthesis of benzo[c][1,7]naphthyridin-4(3H)-ones. Synthesis 2017;49(16):3700–9. https://doi.org/10.1055/s-0036-1590470.

[24] Kulakov IV, Matsukevich MV, Levin ML, Palamarchuk IV, Seilkhanov TM, Fisyuk AS. Synthesis of the first representatives of thieno[3,2-c][1,7]naphthyridine derivatives based on 3-amino-6-methyl-4-(2-thienyl)pyridin-2(1H)-one. Synlett 2018;29(13):1741–4. https://doi.org/10.1055/s-0037-1610445.

[25] Shatsauskas AL, Abramov AA, Chernenko SA, Kostyuchenko AS, Fisyuk AS. Synthesis and photophysical properties of 3-Amino-4-arylpyridin-2(1H)-ones. Synthesis 2020;52:227–38. https://doi.org/10.1055/s-0039-1690231. 02.

[26] Williams ATR, Winfield SA, Miller JN. Relative fluorescence quantum yields using a computer-controlled luminescence spectrometer. Analyst 1983;108:1067–71. https://doi.org/10.1039/an9830801067.

[27] Allen MW. Technical Note: 52019. Measurement of fluorescence quantum yields. Madison(WI): Thermo Fisher Scientific; 2010.

[28] Kostyuchenko AS, Zheleznova TY, Stasyuk AJ, Kurowska A, Domagala W, Pron A, et al. Synthesis and optical Properties of new 5'-aryl-substituted 2,5-bis(3-decyl-2,2'-bithiophen-5-yl)-1,3,4-oxadiazoles. Beilstein J Org Chem 2017;13:313–22. https://doi.org/10.3762/bjoc.13.34.

[29] Kurowska A, Zassowski P, Kostyuchenko AS, Zheleznova TY, Andryukhova KV, Fisyuk AS, et al. Effect of donor to acceptor ratio on electrochemical and spectroscopic properties of oligoalkylthiophene 1,3,4-oxadiazole derivatives. Phys Chem Chem Phys 2017;19:30261–76. https://doi.org/10.1039/C7CP05155G.

[30] Shatsauskas AL, Mamonova TE, Stasyuk AJ, Chernenko SA, Slepukhin PA, Kostyuchenko AS, et al. A rearrangement of 7-aryloxazolo[5,4-b]pyridines to benzo[c][1,7]naphthyridine-4(3H)-ones and thieno[3,2-c][1,7]naphthyridine-6(7H)-ones. J Org Chem 2020;85(15):10072–82. https://doi.org/10.1021/acs.joc.0c01299.

[31] Tsypko TG, Petrakova IS, Brilenok NS, Nikolaeva NA, Chuprinina DA, Temerdashev ZA, et al. Determination of total content of antioxidants by FRAP assay. Analitika i control 2011;15(3):287–9 [Russian].

[32] Brilenok NS, Vershnin VI, Bakhareva MV. Evaluation of polyphenols antioxidant capacity in the presence of complexants by FRAP assay. Analitika i control 2016;20(3):209–17. https://doi.org/10.15826/analitika.2016.20.3.004. Russian.

[33] Azevedo AM, Martins VC, Prazeres DMF, Vojinović V, Cabral JMS, Fonseca LP. Horseradish peroxidase: a valuable tool in biotechnology. Biotechnol Annu Rev 2003;9:199–247. https://doi.org/10.1016/S1387-2656(03)09003-3.

[34] Zhang Sh, Garcia-D'Angeli A, Brennand JP, Huo Q. Predicting detection limits of enzyme-linked immunosorbent assay (ELISA) and bioanalytical techniques in general. Analyst 2014;139:439–45. https://doi.org/10.1039/C3AN01835K.

[35] Cai H, Liu X, Zou J, Xiao J, Yuan B, Li F, et al. Multi-wavelength spectrophotometric determination of hydrogen peroxide in water with peroxidase-catalyzed oxidation of ABTS. Chemosphere 2018;193:833–9.

[36] Watabe S, Sakamoto Y, Morikawa M, Okada R, Miura T, Ito E. Highly sensitive determination of hydrogen peroxide and glucose by fluorescence correlation spectroscopy. PloS One 2011;6(8):e22955. https://doi.org/10.1371/journal.pone.0022955.

[37] Corley J. Best practices in establishing detection and quantification limits for pesticide residues in foods. In: Lee P, editor. Handbook of residue analytical methods for agrochemicals. West Sussex: John Wiley and sons; 2003. p. 59–75.

[38] Paul KG, Stigbrand T. Four isoperoxidases from horse radish root. Acta Chem Scand 1970;24:3607–17. https://doi.org/10.3891/acta.chem.scand.24-3607.

[39] Nelson DP, Kiesow LA. Enthalpy of decomposition of hydrogen peroxide by catalase at 25° C (with molar extinction coefficients of H2O2 solutions in the UV). Anal Biochem 1972;49(2):474–8. https://doi.org/10.1016/0003-2697(72)90451-4.